Vertical jumping in *Galago senegalensis*: the quest for an obligate mechanical power amplifier

Peter Aerts

Department of Biology, University of Antwerp (UIA), Universiteitsplein 1, B-2610 Wilrijk, Belgium

Bushbabies (*Galago senegalensis*) are renowned for their phenomenal jumping capacity. It was postulated that mechanical power amplification must be involved. Dynamic analysis of the vertical jumps performed by two bushbabies confirms the need for a power amplifier. Inverse dynamics coupled to a geometric musculo-skeletal model were used to elucidate the precise nature of the mechanism powering maximal vertical jumps. Most of the power required for jumping is delivered by the vastus muscle–tendon systems (knee extensor). Comparison with the external joint-powers revealed, however, an important power transport from this extensor (about 65%) to the ankle and the midfoot via the bi-articular calf muscles. Peak power output likely implies elastic recoil of the complex aponeurotic system of the vastus muscle. Patterns of changes in length and tension of the muscle–tendon complex during different phases of the jump were found which provide strong evidence for substantial power amplification (×15). It is argued here that the multiple internal connective tissue sheets and attachment structures of the well-developed bundles of the vastus muscle become increasingly stretched during preparatory crouching and throughout the extension phase, except for the last 13 ms of the push-off (i.e. when power requirements peak). Then, tension in the knee extensors abruptly falls from its maximum, allowing the necessary fast recoil of the tensed tendon structures to occur.

Keywords: *Galago senegalensis*; jumping mechanism; power amplification; inverse dynamics

1. INTRODUCTION

In assessing the mechanical capabilities of musculo-skeletal systems, the analysis of maximal jumping is exemplary, as the natural demands imposed on the system are maximized too (see, for example, Sellers 1992). The involved stresses are high and impact-like (cf. Bennet-Clark 1976, 1977), and the energy required for every new leap has, theoretically, to be delivered *de novo* by the muscles (see, for example, Bennet-Clark 1976, 1977; Günther *et al.* 1991; Crompton *et al.* 1993). In his theoretical analyses on the energetics of jumping and the effects of size, Bennet-Clark (1976, 1977) noted that animals, perfectly capable of delivering the jumping energy instantaneously, can have difficulties when the rate at which the work has to be done to attain a certain height exceeds the muscle power. In other words, instantaneous power output capabilities of muscles can constrain jumping performance. This is primarily true for the smaller animals, as the power that is instantaneously required is directly proportional to the available acceleration distance (i.e. leg length in most of the cases). Therefore, jumpers might benefit from a mechanical power amplifier that releases previously stored energy at an increased rate (see, for example, Bennet-Clark 1976, 1977; Emerson 1985; Alexander 1992).

The bushbaby *Galago senegalensis* (Lorisiformes) is well-known for its enormous jumping capabilities (see, for example, Hall-Craggs 1964, 1965, 1974; Jouffroy & Gasc 1974; Jouffroy *et al.* 1974; Günther & Niemitz 1982; Jouffroy & Günther 1985; Günther 1985, 1989; Jouffroy 1989; Demes & Günther 1989; Günther *et al.* 1991, 1992; Sellers 1992; Crompton *et al.* 1993). The highest reliably reported vertical jump for a 0.250 kg animal is 2.25 m (Hall-Craggs 1965), which corresponds to a displacement of the centre of gravity during the flight phase of approximately six body lengths (tail not included). Based on this information, and assuming a constant acceleration during the push-off, Bennet-Clark (1976) estimated a specific power output of 2350 W per kilogram of muscle, provided that the jump is instantaneously powered by the contractile components of the muscles. (It was assumed that 40% of the body mass consists of muscles involved in jumping.) Such a value is well above the maximally attainable output deduced for vertebrate muscle (for example, 860 W kg^{-1} theoretical maximum for pigeon flight muscles (Pennycuick & Parker 1966); 270–371 W kg^{-1} calculated and measured for frog hindlimb muscles (Lutz & Rome 1994; Marsh & John-Alder 1994); 380 W kg^{-1} for typical fast glycolitic fibres (based on data presented in Herzog (1994))). Such considerations encouraged Bennet-Clark to infer that energy storage for power amplification is likely to occur also in bushbabies. Later, this discrepancy between power requirements for jumping and specific power output of muscles was confirmed experimentally by Günther (1985; although not explicitly stipulated). This author accurately determined the external peak power for the acceleration
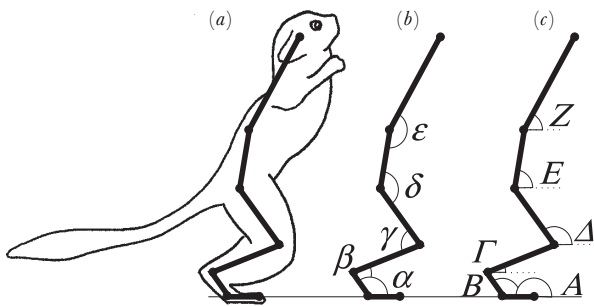
Figure 1. (*a*) Linked segment model with respect to an outline drawing of a jumping bushbaby. (*b*) Internal joint angles (joint extension accords to their increase; see text). (*c*) External joint angles (with respect to the horizontal). Joint labels are used in the equations of figure 2.

of the centre of gravity of a 0.280 kg bushbaby (based on the registration of ground reaction forces during the push-off for a leap equivalent to a 1.5 m vertical jump). The power peak of 191 W recalculates to about 1700 W kg^{-1} (assumptions about muscle mass accords to Bennet-Clark (1976)). Also Jouffroy & Gasc (1974) and Jouffroy & Günther (1985) postulated that elastic rebound of ligaments and tendons provides energy for the jump, however, without reference to the possibly increased power output.

Despite the evidence for a mechanical power amplifier being present in *Galago senegalensis*, its precise nature (if it exists at all!) remains obscure. In this paper, an inverse dynamical analysis is done (cf. Winter 1990) to gain more insight into jumping by bushbabies. The power freed externally at the level of the extending joints is calculated as a function of time (i.e. the external power distribution) and related to the power production by muscle−tendon complexes (i.e. the internal power distribution). Assessing tension and/or length profiles of muscle−tendon complexes permits us to draw conclusions about the appearance, role and relevance of power amplifying mechanisms which allow bushbabies to jump as they do.

2. MATERIALS AND METHODS

(a) *Study specimens and experimental set-up*

The two bushbabies (*Galago senegalensis braccatus*; mass: sp.1 = 0.251 kg and sp.2 = 0.306 kg; extended snout−toe length: sp.1 = 0.35 m and sp.2 = 0.34 m) used in this study were purchased from the zoological garden of Emmen (The Netherlands), and were kept at the Antwerp Zoo (Royal Zoological Society, Antwerp), where experiments took place. Symmetrical vertical jumps were videotaped simultaneously at 500 Hz (NAC-1000; illumination: 6 kW; field of view: specimens at push-off) and at 50 Hz (Panasonic MS1-sVHS; field of view: entire jump). Ground reaction forces in vertical (Z), lateral (X) and front-aft (Y) direction and the position of the centre of pressure (X,Y) were measured simultaneously by means of a KISTLER 9281 Bll force plate (with KISTLER 5001 amplifiers) and stored on magnetic tape (Honeywell, 5600C). For synchronization, an asymmetrical square pulse (TEKTRONIX, TM503; 9.05 Hz), also driving an LED visible on the video images, was stored together with the force data.

(b) *Analysis*

Force signals were digitized at 4 kHz (Intelligent Meβ-technik, TI2840). A total of 21 jumps were retained (Plompen *et al.* 1992) for which transversal forces were negligible (i.e. symmetrical jumps; perpendicular to the camera) and for which the angle between the peak ground reaction force and the horizontal plane exceeded 75° (i.e. nearly vertical jumping). The instantaneous acceleration, a_t, of the centre of gravity of the animal along its path was calculated from the forces:

$$a_t = (F_{X_t}^2 + F_{Y_t}^2 + (F_{Z_t} - mg)^2)^{1/2}/m, \tag{1}$$

where: m is total mass of the animal, g is acceleration of gravity, $F_{X,Y,Z}$ are components of the ground reaction forces). The instantaneous velocity was calculated by numerical integration of the acceleration. The vector sum of the three force components multiplied by the instantaneous velocity gave the power needed for the observed displacement of the centre of gravity during the push-off phase (i.e. centroid power).

For this study, the highest jump of each specimen was selected for further analysis. In this way, individual maximized performance was assessed. Specimen 1 reached a height of 1.74 m (code, J33: force angle at take-off = 84°); specimen 2 jumped 1.42 m (code, J26: force angle at take-off = 85°). The specimens were represented by a linkage of six rigid segments (see figure 1), defined by the lateral view coordinates of the tip of the longest toe, the tarso-metatarsal joint (midfoot joint), the ankle, the knee, the hip, the middle of the backbone and the centre of the head (figure 1). These body points were digitized frame by frame by using the NAC1000 XY-coordinator and MOVIAS- and purpose-written software. Coordinates were recalculated according the scaling and perspective of the video images. As the selected jumps were symmetrical, left- and right-leg segments were represented by one link.

For each frame, the two-dimensional position of the centre of gravity (CG) of the links was calculated (see table 1) based on the data presented by Smith (1987, tab. 4: positions of the CG as a fraction of the segment length from the proximal end to the CG).

Further, the angle between each link and the horizontal was determined frame by frame (i.e. external angles; they are defined counterclockwise for specimens facing to the right; see figure 1*a*). Intersegmental angles (i.e. internal angles) were determined in such a manner that joint extension coincided with their increase (see figure 1*b*).

Noise on linear and angular positional data was suppressed by means of a zero-phase shift digital low-pass filter. The cut-off frequency was adjusted until the acceleration obtained by double numerical differentiation was free of noise. The software code was supplied by G. A. Wood, Department of Movement Studies, University of West Australia (see Wood 1982). This code also provided the angular and linear velocities and accelerations.

(c) *Inverse dynamics*

Based on the kinematical data and the ground reaction forces, instantaneous net joint moments were calculated (i.e. the instantaneous moments required in each joint to sustain the observed body movements). These calculations

Table 1. *Morphometric data for specimens 1 and 2*

(up.trk., upper trunk; low.trk., lower trunk; low.leg, lower leg; CG, position of the centre of gravity (as a percentage of total segment length) measured from the upper end of the segment; MOI_{CG}, moment of inertia with respect to the centre of gravity.)

	specimen 1				specimen 2			
	length (m)	mass (kg)	CG (%)	MOI_{CG} (kg m^{-2})	length (m)	mass (kg)	CG (%)	MOI_{CG} (kg m^{-2})
up.trk.	0.088	0.098	49	5.11×10^{-4}	0.082	0.119	49	6.60×10^{-4}
low.trk.	0.024	0.033	53	2.36×10^{-4}	0.027	0.040	53	2.83×10^{-4}
thigh	0.069	0.075	46	2.17×10^{-5}	0.069	0.092	46	2.72×10^{-5}
low.leg	0.067	0.030	40	6.00×10^{-6}	0.067	0.037	40	1.53×10^{-6}
hindfoot	0.025	0.005	57	3.80×10^{-7}	0.026	0.006	57	4.50×10^{-7}
forefoot	0.029	0.010	48	2.25×10^{-6}	0.029	0.012	48	2.80×10^{-6}

relied on the solution of the instantaneous sets of equations of motion in two dimensions (i.e. planar segmental movements were assumed) for each segment:

$$\Sigma F_{Y,Z} = ma_{Y,Z}, \tag{2}$$

$$\Sigma M_X = I_X \alpha_X, \tag{3}$$

where $F_{Y,Z}$ are external forces (ground–joint reaction forces, gravity) in both directions; $a_{Y,Z}$ are linear accelerations of the centre of gravity; M_X are moments exerted by all $F_{Y,Z}$'s about the CG; I_X is moment of inertia about the CG; α_X is angular acceleration about the CG). Moments that must be introduced to fulfil equation (3) are assumed to be the net result of the stresses occurring in muscle–tendon complexes crossing the specific segmental joints (for more information on inverse dynamics, see Zajac & Gordon (1989); Winter 1990; Enoka 1994; Nigg & Herzog 1994; Zernicke & Smith 1996). The required morphometric data are summarized in table 1. Segment masses and moments of inertia were recalculated from experimentally determined data presented by Smith (1987, tab. 5 and 6) for a 0.310 kg *Galago senegalensis braccatus*. Isometric scaling was assumed. These data (see table 1) largely compare to those presented by Sellers (1992).

The equilibrium was first calculated for the distal-most segment (i.e. distal foot segment which equals the forefoot) on which the ground reaction forces applied. The precision of the position of the point of application as supplied by the force plate was inadequate early in the push-off (only provided when vertical force components exceed 10% of the full-scale setting; the signal was too noisy). Therefore, calculations were only done for approximately the last 60 ms of the push-off during which only the forefoot contacts the force plate (i.e. the heel is lifted from the ground). Except for the last 10 ms, ground reaction forces were assumed to apply centrally on the forefoot. For the last 10 ms the point of application was shifted linearly in time towards the toe tip, because then the forefoot pivoted too. (A sensitivity analysis proved that shifting the position of the point of application beneath the part of the foot contacting the ground does not affect the conclusions drawn from this study.) Once the equilibrium for the forefoot was solved, calculations could be done for the hind foot, then for the

lower leg, and so on. Judging the small masses of the distal-most links (see table 1), this bottom–top approach (with measured ground reaction forces introduced) ensures reliable results for the net moments of the distal joints (midfoot, ankle, knee). Net joint–moments tending to extend the joint were considered positive.

These moments were then used to calculate net joint powers (power is the mechanical work done per unit of time) by multiplying them with the instantaneous angular velocities of the internal joint angles. Joint powers were summed for all joints and compared with the centroid power as deduced from the ground reaction forces.

(d) *Geometric musculo-skeletal model*

Morphological and morphometric data were gathered from the literature (Hall-Craggs 1966, 1974; Stevens *et al.* 1971, 1972, 1981; Grand 1977; Alexander *et al.* 1981; Günther 1989) and from the dissection of a preserved specimen (0.132 kg, extended length = 0.27 m; i.e. isometrically scaled with the test specimens). Attention was paid to relative muscle masses and to tendons and connective tissue structures within the muscles. Distances between muscle attachment sites and joint centres were measured and isometrically scaled to the size of the experimental animals (linear dimensions were considered identical for both specimens; cf. total lengths mentioned here). This information was used to frame a simple geometric model (figure 2) which allowed estimation of the length changes and tension profiles for three extensor muscle–tendon complexes (vastus, bi-articular calf muscles and plantar aponeurosis; see figure 2 and table 2). For the deductive analysis, net joint moments at the tarso-metatarsal joint and the ankle were assumed to be generated solely by the plantar aponeurosis (the most important structure at the plantar side of the foot, Stevens *et al.* (1972); Plompen 1992) and bi-articular calf muscles (which equals gastrocnemius plus plantaris, sharing the Achilles tendon and their attachment at the femur and constituting more than 90% of the extensor mass of the ankle; Plompen 1992), respectively. At the knee, it is assumed that only the vastus muscle group (which constitutes about 53% of the mass of all leg muscles or 12.5% (both legs) of the body mass; Plompen 1992) delivers the extension force. The slender, bi-articular, rectus femoris muscle (only about 1% of the leg
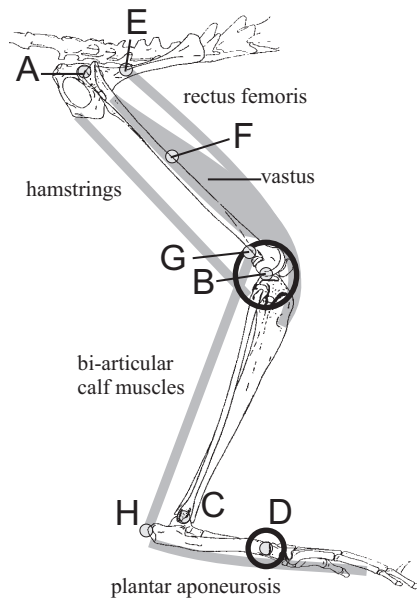
Figure 2. Geometric musculo-skeletal model of the hind leg of *Galago senegalensis*. (Skeletal parts are modified after Stevens *et al.* (1971).) F_{plant}, midfoot moment/D_{radius}; F_{gast}, ankle moment/($HC \times \sin(\beta)$); F_{vastu}, ($F_{gast} \times \sin(\gamma) \times BG$+knee moment)/$D_{radius}$; ΔL_{plant}, $-\Delta\alpha D_{radius}$; ΔL_{gast}, $-\Delta[(CB \times \sin(r) - CH \times \sin(B) + BG \times \sin(\Delta))^2 + (CB \times \cos(r) - CH \times \cos(B) + BG \times \cos(\Delta))^2]^{.5}$; L_{vastu}, $-\Delta\gamma \times B_{radius} \Delta L_{rectu}$, $-\Delta\gamma \times D_{radius} + \Delta\delta \times AE$. F_{plant}, F_{gastr} and F_{vastu} refer to the tension of the plantar aponeurosis, the bi-articular calf and vastus muscle–tendon complexes, respectively. The other equations give the length changes of the muscle–tendon complexes (L_{rectu}: rectus femoris). B_{radius} and D_{radius} refer to the radius of the pulley of joint B and D, respectively. Numerical data are given in table 2.

muscle mass) could not be considered in the tension estimates as it would make the system indeterminate. It is argued (see further) that the hamstrings are not active during knee extension. Thus, the net knee moment was assumed to be the result of the combined activity of the bi-articular calf muscles and the vastus-part of the quadriceps femoris.

About the hip, many muscles, apart from the hamstrings, can contribute to the net joint moment and no morphological and morphometric arguments can be put forward to assign this moment primarily to only one of these muscles. Furthermore, the important and fast elevation and extension of the trunk is likely caused by rotations in all the vertebral articulations. The two trunk segments are introduced to assess vaulting of the back but do not accord to any specific morphological unit. For these reasons, calculations of muscle stress about the hip and the back joint are questionable and were not done here.

The moment arms of the calf muscles at the ankle and knee varied according to the instantaneous configuration of the model (see figure 2). The moment arm of the vastus muscle at the knee and that of the plantaris aponeurosis at the midfoot joint were kept constant (as if acting along a pulley; see figure 2). For the rectus femoris only length changes were estimated (see figure 2). A positive slope in the curve for length (see figure 7) corresponded to muscle shortening, whereas a negative slope corresponded to lengthening. This allowed for positive shortening

Table 2. *Numerical data for the geometric muscle–tendon model*

(See figure 2.)

	description	distance (m)
A–E	hip: insertion rectus femoris	0.0100
B–F	knee: insertion vastus	0.0300
B–radius	radius 'knee-pulley' (see text)	0.0040
B–G	knee: insertion gastrocnemius on femur	0.0050
C–H	ankle: insertion gastrocnemius on heel	0.0070
H–D	length tarsus	0.0230
D–radius	radius 'midfoot-pulley' (see text)	0.0025

velocities. Muscle–tendon length at the onset of the inverse dynamics calculations was arbitrarily used as the reference length (i.e. zero shortening–extension).

Differentiation of muscle lengths gave shortening–lengthening velocities, and approximate muscular power output (i.e. internal power) was calculated from the product of contraction force and speed. Positive shortening velocities yielded positive power output during concentric contraction.

As mentioned, inverse dynamics and musculo-skeletal modelling are done for the highest jumps obtained for each of the experimental animals. It is assumed that maximized individual performance can be assessed in this way. Comparison of the results of both specimens thus allows evaluation of the general validity of the conclusions drawn from the deductive modelling. Therefore, the model outputs (inverse dynamics and geometric model) of J33 (specimen 1) and J26 (specimen 2) are presented in parallel. In all graphs, zero-time coincides with the instant the animal leaves the force plate.

3. RESULTS AND DISCUSSION

(a) *Inverse dynamics and power requirements*

Displacement and ground reaction force profiles are stereotyped and compare satisfactorily with formerly published kinesiological descriptions to which we referred for details (Hall-Craggs 1964, 1965; Jouffroy & Gasc 1974; Günther & Niemitz 1982; Günther 1985, 1989; Jouffroy & Günther 1985; Demes & Günther 1989; Günther *et al.* 1991, 1992). The ground reaction forces and the internal angles of J33, being a typical example of a maximized vertical jump of the bushbaby, are presented in figure 3 and are used as a reference for further discussion.

The results of the inverse dynamics analysis for the last 60 ms of the push-off are given in figures 4, 5 and 6. Except for the last few milliseconds of knee extension, all net joint moments needed to sustain the observed movements were positive (i.e. tending to extend the corresponding joint) and increase towards the ultimate phase of the push-off where ground reaction forces peak (compare figure 4 with figure 3a). As well as the highest moments (figure 4), also the most power is freed externally at the level of the ankle (about two-fold of the knee peak-power; figure 5). The power output at the level of the hip and the back is more or less constant and low
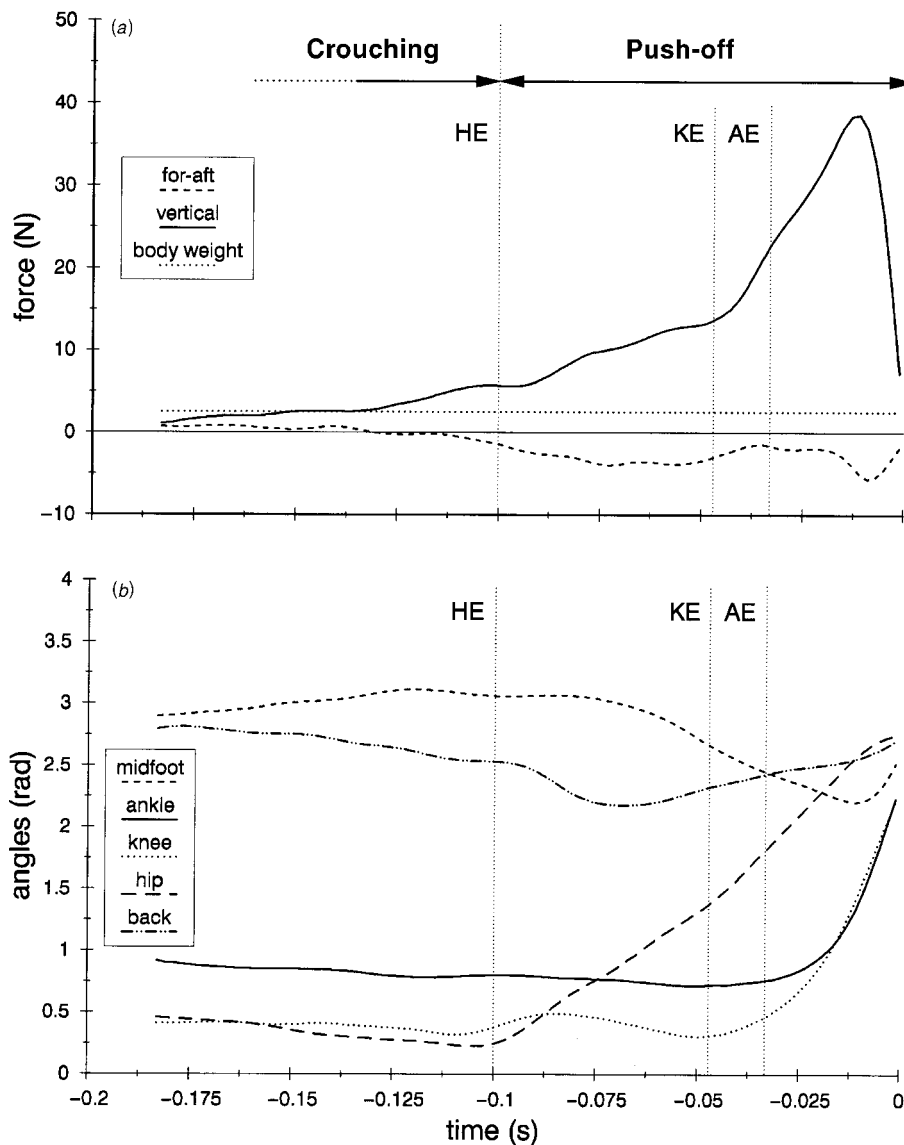
Figure 3. (*a*) Vertical and for–aft ground reaction forces of jump J33. Zero-time coincides with take-off. At −0.1 s, the push-off initiates (see text). For this jump, crouching lasts about 350 ms. The dotted line represents body weight. Negative fore–aft forces represent backwards pushing. (*b*) According angular displacement profiles of the joints between the body segments. (AE: onset of ankle extension; HE: onset of hip extension; KE: onset of knee extension).

compared with that at the ankle and knee. Energy is absorbed (negative power; figure 5) at the midfoot joint during the main part of the push-off because the joint is flexed (see figure 3*b*) against an extending moment (figure 4). But, during the fast ultimate extension of this joint, power output becomes positive too. Ultimate braking of the knee extension also involves energy absorption (negative power; see also final knee flexing moment in figure 4).

Figure 6 compares the summed joint powers with the mechanical power needed to move the centroid along its path during the push-off (i.e. centroid power). (Theoretically, these curves must be nearly identical as internal work can safely be assumed to be a small fraction of the total mechanical costs.) Despite the many simplifications intrinsic to the inverse dynamics procedure and the fact that the test specimens could not be manipulated or sacrificed (among others: representation by limited number rigid segments; digitization of unmarked body points; extrapolation of morphometric data from the literature and so on), the shape of the profile and the timing and amplitudes of the peaks coincide quite well. This, together with the agreement of

the global image of the joint power profiles between J33 and J26 (figure 5) and the similarity of the moment curves for the specific joints (figure 4), supports the general relevance and validity of the results of the kinematical and dynamical analysis.

The high power requirements for the jumps of bushbabies as predicted by Bennet-Clark (1977) and reported by Günther (1985) (see §1) are thus confirmed by the present results. Based on the peak centroid power (200 W) and making use of the highest actually measured specific instantaneous power output for vertebrate skeletal muscle (371 W kg^{-1} muscle: semimembranosus muscle of *Rana pipiens*; Lutz & Rome 1994), specimen 1 should need 0.539 kg of extensor muscle to power its J33 jump instantaneously by concentric activity of the contractile components of these muscles. For J26 of specimen 2 this value is 0.477 kg. Given the body mass of each animal (0.250 and 0.306 kg, respectively) and the fact that the leg muscles amount to about 25% of this, *Galago*'s jumping muscles should perform six to nine times better than the frog's semimembranosus muscle. One argument could be that mammalian skeletal muscles perform better than those of amphibians. This, however, is not
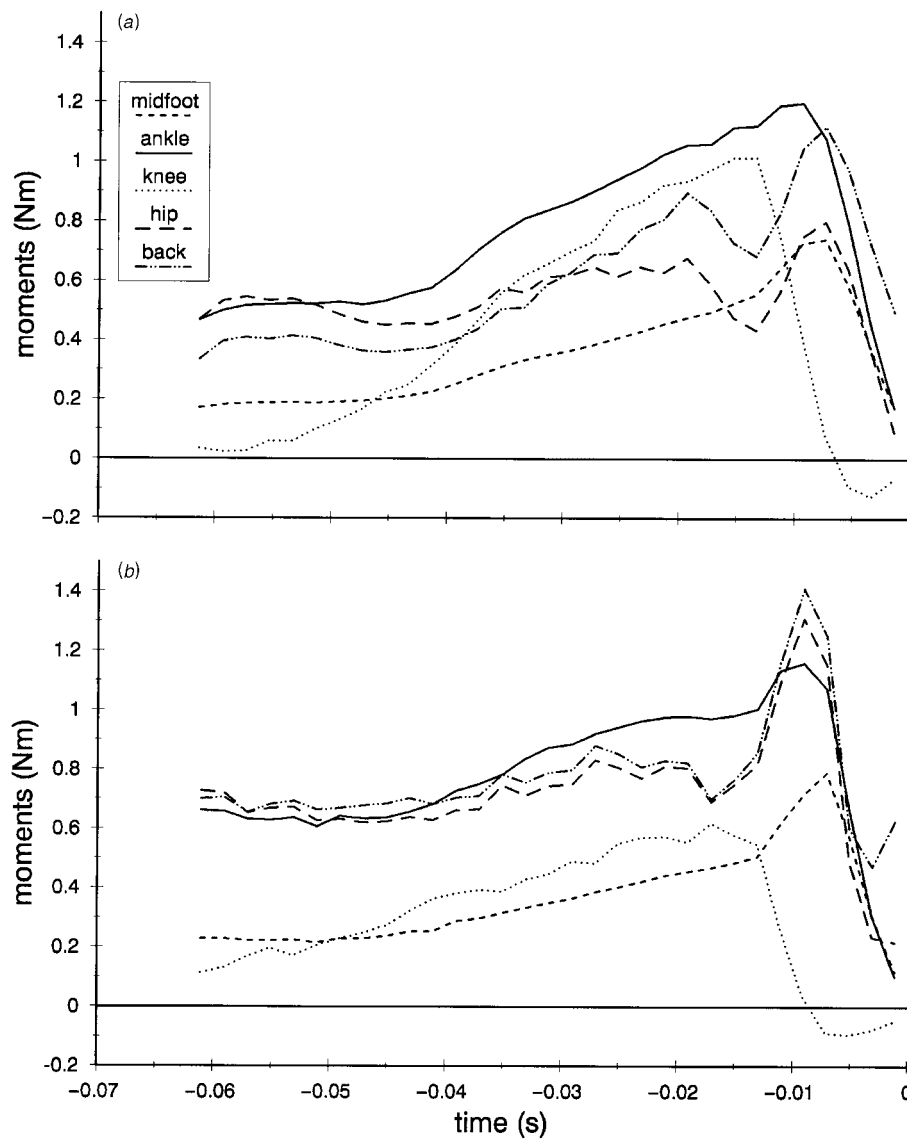
Figure 4. (*a*) Nett moments required at the joints to sustain the observed segmental movements of jump J33. (*b*) As in (*a*) but for jump J26

very plausible because muscle stress (25 N cm^{-2}) and shortening speed (16 fibre lengths per second) of fast glycolitic mammalian muscle fibres as presented by Herzog (1994; based on a variety of literature sources), results in a maximum of 380 W kg^{-1} muscle (based on equation 2.5.19 in Herzog (1994)), being pretty close to the measured optimal performance of the amphibian hamstring. Even with the theoretical maximum of 860 W kg^{-1} inferred for pigeon flight muscle (Pennycuick & Parker 1966; based on the breaking strength of the insertion), the bushbaby obviously needs a mechanical power amplifier for its maximal jumping.

Mechanical power amplification occurs when elastic strain energy (stored in an initial phase of the jump) is released at an increased rate. Stretched ligaments, tendons and aponeuroses can function in this way (Alexander 1988), but also elastic recoil of the muscle fibre itself (Alexander & Bennet-Clark 1977: cross bridge elasticity; sarcolemma) potentially contributes to an increase in power output. Alexander & Bennet-Clark (1977) noted, however, that for mammal locomotion, the contribution of muscle elasticity is small compared with that of tendon (ligament) elasticity.

In a recent model, Alexander (1995) evaluates the performance of different jumping techniques, in relation to the size of the jumper and (among others) to the tendon compliance. In a catapult jump, muscles work nearly isometrically in deforming serially arranged elastic structures (tendons, apodemes, and so on). A trigger suddenly releases the stored energy to power the push-off. The second technique, the countermovement jump, mimics, in a certain way, the energy storage occurring during cyclic movements (see, for example, Alexander 1988, 1992). The body first moves downwards (gravitation plus muscle activity), to proceed immediately in the upwards acceleration for the push-off. The effect is two-fold. Activated muscle–tendon complexes are stretched and loaded with elastic energy by braking the down-wards-moving body (conversion of kinetic energy), and/ or by co-contraction of antagonists (see, for example, Van Leeuwen 1992). Furthermore, muscles in an activated stretch–shortening cycle show a substantial increase of the intrinsic power output during the concentric phase (i.e. muscle potentiation; see, for example, Komi 1992; Woledge *et al*. 1985). To benefit from elastic recoil, catapults and countermovement jumps must show
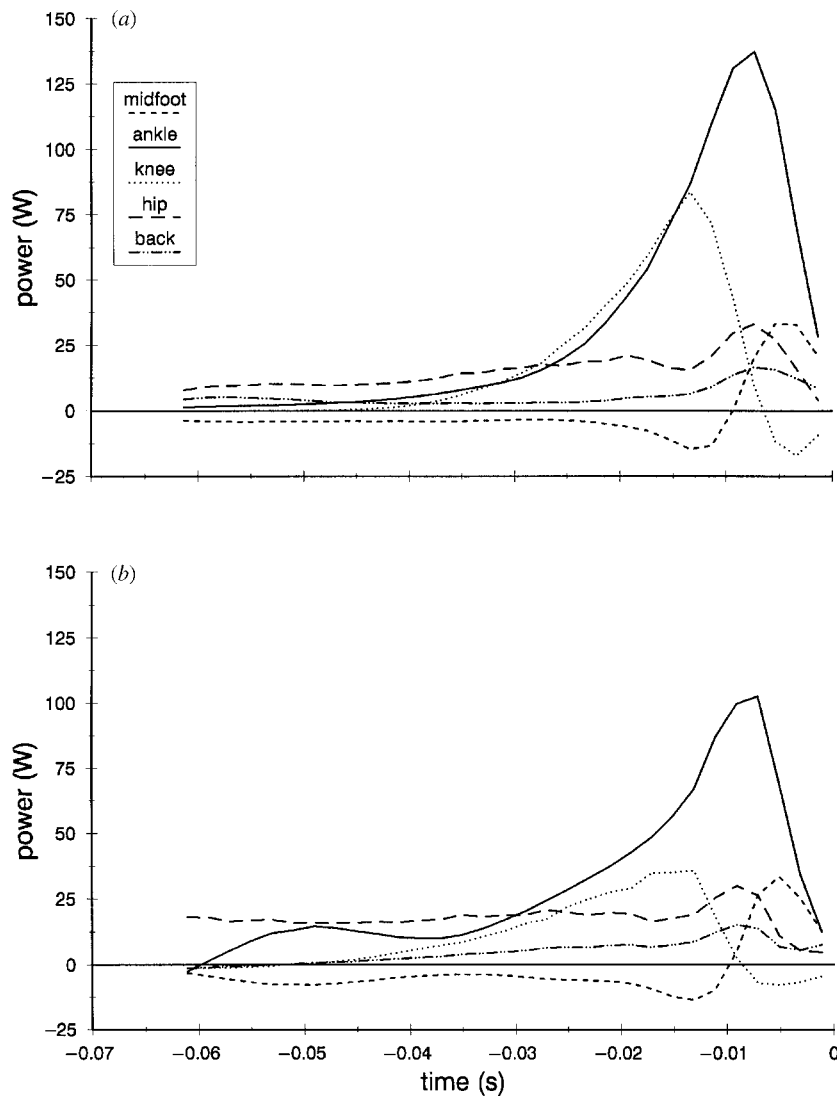
Figure 5. (*a*) Net power output at the joints (which equals external power) to sustain the observed segmental movements of jump J33. (*b*) As in (*a*) but for jump J26.

maximal muscle torques when joint extension for the push-off (upwards acceleration) starts. This contrasts with squat jumping where muscle forces are minimal at the onset of the push-off and mount to a maximum well before the extension phase ends (Alexander 1995). As long as the muscle force increases, serially arranged tendons are strained by the shortening muscle. Tendon recoil occurs when muscle force drops again. For all three techniques, it will depend on the compliance of the strained components and the specific loading pattern whether or not power amplification occurs.

For a bushbaby-sized animal, the model (Alexander 1995) predicts that the potential benefit from a counter-movement is small compared with that of a catapult, whereas performance in squat jumping (with similar tendon compliance) has the least benefit of all. However, catapults do not seem to have evolved in mammals (Crompton *et al.* 1993; Alexander 1995). Furthermore, despite the presence of countermovements (see figure 3*a,b*: crouching; ground reaction forces below body weight; see also Hall-Craggs 1965; Günther 1985, 1989), their effectiveness in terms of using strain energy must be doubted too. Muscle stresses must be about maximal when the deepest position in the countermovement is

reached (Alexander 1995; cf. human jumping: P. Aerts, personal observations; Bobbert *et al.* 1986*a*). The ground reaction force records reveal that this condition cannot be fulfilled in the jump of the *Galago*. At the onset of exten-sion, the ground reaction force amounts to only about 15% of its peak value (contrary to human jumping where it is nearly maximal at that instant). Therefore, it must be concluded that the extreme crouching of the bushbaby mainly serves to increase the available acceleration distance during push-off.

Yet, the arguments here definitely point at a power amplifying mechanism. Studying the manner in which muscle–tendon systems produce the power externally required at the level of the joints will help us to under-stand it.

(b) *Geometric musculo-skeletal model and power amplification*

Figure 7 shows the length changes of the muscle–tendon complexes during the last 63 ms of the push-off. For the vastus and the bi-articular calf muscles, these profiles do approximate the length changes for the entire push-off, because the involved joint angles start to extend late (in about the last 50 ms; see figure 3*b*). The same
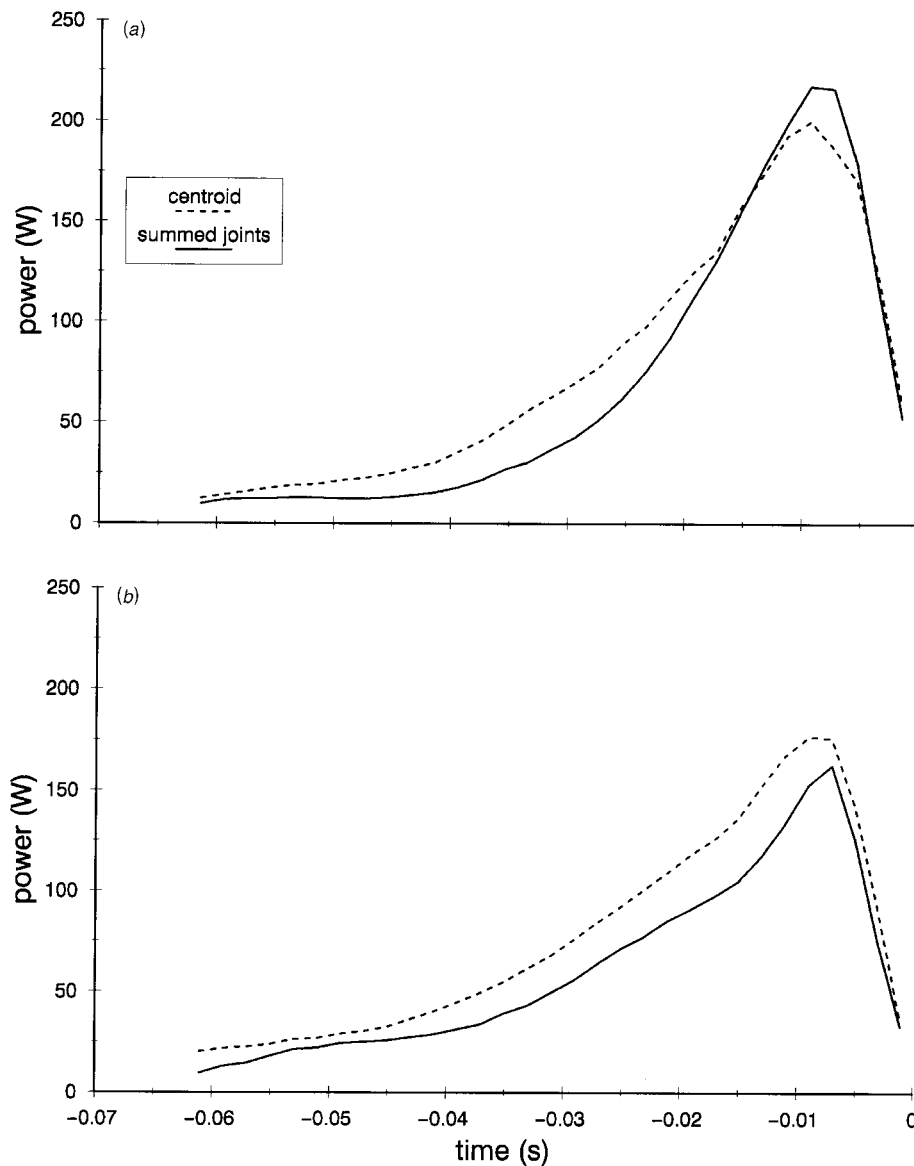
Figure 6. (*a*) Comparison of the summed net joint powers with the power needed to displace the centre of gravity (centroid power; calculated from the ground reaction forces) of jump J33. (*b*) As in (*a*) but for jump J26.

holds true for the plantar aponeurosis. Flexion of the midfoot joint initiates immediately before the onset of the model simulations (see figure 3*b*). Because the hip extension initiates well before the onset of the simulations (see figure 3*b*), it is obvious that the rectus femoris shows its shortest length when the animal is completely crouched.

Figure 8 gives the tension of the vastus and bi-articular calf muscle–tendon complexes and of the plantar aponeurosis. For the vastus muscle, the required tension sharply increases, to peak about 15 ms before take-off. From these very high peak-forces (about 480 N in J33) tension rapidly drops to zero at take-off. The same pattern is observed for the plantar aponeurosis, but maximum tension (about 250 N for both jumps) is considerably lower than for the vastus muscle. For the calf muscles, tension remains more or less constant.

Figure 9 represents the power output by the retained extensor systems (internal power output). They peak in a proximo-distal sequence: first the vastus, then the calf muscles and finally the plantar aponeurosis. Although externally the power output is highest at the level of the ankle joint (see figure 5), it is the vastus muscle–tendon

complex (knee extensor) which delivers internally most of the required power. As predicted earlier, power is absorbed by the plantar aponeurosis (negative power) because the midfoot-joint is flexed (as a result of backwards trunk accelerations and ankle extension) against an extending moment. This stored energy is released during the last 10 ms of the push-off.

Comparison of the positive and negative power peaks calculated for the midfoot joint (or the plantar aponeurosis; figures 5 and 9) shows that there is a $\times 2.5$ amplification factor. However, the positive power delivered by the aponeurosis maximally contributes only 16–18% to the overall instantaneous power peak (compare figures 5 and 6). Therefore, it is concluded that the role of the fast extension of the distal foot segments is to ensure prolonged acceleration late in the push-off. In reality, an extra joint is present in the forefoot segment (between the metatarsals and the first large phalanges; Stevens *et al.* 1971) which also shows a flexion–extension mechanism similar to that of the midfoot joint, but with the fast extension postponed still further to the last few milliseconds of the push-off. Probably, the latter extension
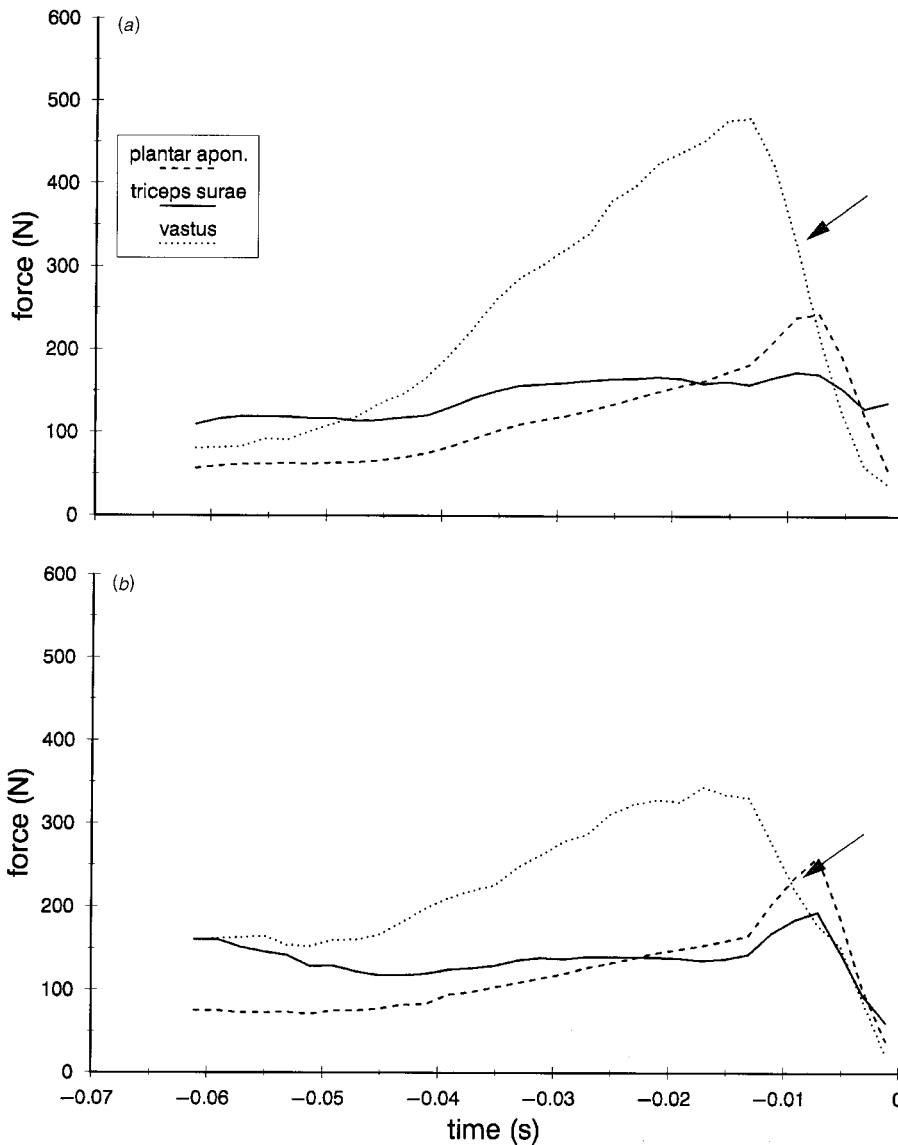
Figure 7. (*a*) Length changes of the considered muscle–tendon complexes during the last 63 ms of the push-off of jump J33. (*b*) As in (*a*) but for jump J26.

movement also minimizes deceleration when the ground reaction force drops below body weight, although this function is of minimal importance because this period is extremely small in jumping bushbabies (less than 0.5 ms; see figure 3*a*).

Thus, power amplification is most likely to be found at the level of the knee or ankle. Externally, most power is delivered at the ankle (up to 68% of the centroid power peak; see figure 5). Less power is produced at the knee (figure 5). Internally, however, the reverse is true: by far most of the energy for the jump is delivered by the knee extensors (the vastus muscle) and not by the ankle extensors. This inversion implies that the bi-articular calf muscles mainly functions as a link, coupling extension of the knee to that of the ankle. This is confirmed by the results of the muscle–tendon model: the length changes of the calf muscles are small (about 3% of the initial length; see also Hall-Craggs 1965, 1974), occur late in the push-off and their tension remains fairly constant. Hall-Craggs (1965, 1966, 1974) already described this coupling. The energetic consequences, however, were not mentioned: a considerable portion of the energy for jumping released at the ankle comes from concentric

work done by the knee extensors. A similar power transport function is described and quantified for the human bi-articular calf muscles (Bobbert *et al*. 1986*b*; Komi 1992; Jacobs *et al*. 1996). Based on detailed modelling it is concluded that about 25% of the total energy delivered at the ankle is transported from the knee. Our geometric muscle–tendon model is much too simple to allow for precise quantification. It aims to reveal the mechanism of jumping and not to provide us with absolute measures. Nevertheless, comparison of the integrated power profiles of the ankle (external) and the calf muscles (internal) strongly suggests that power transport is of much higher importance in bushbabies (J33: 65%; J26: 60%). As storage of strain energy in the plantar aponeurosis relies, at least partly, on ankle extension, power from the knee extensors is probably transported to the midfoot joint too.

In view of power release for jumping, the conclusions drawn here put the focus on the vastus muscle. Despite its powerful appearance reflected in its mass (53% of the mass of all leg muscles; about 12.5% of the body mass; see also Hall-Craggs 1974), and its fibre composition (up to 87% fast glycolitic fibres; Sickels & Pinkstaff 1981; Stevens *et al*. 1981), a power amplifier still seems
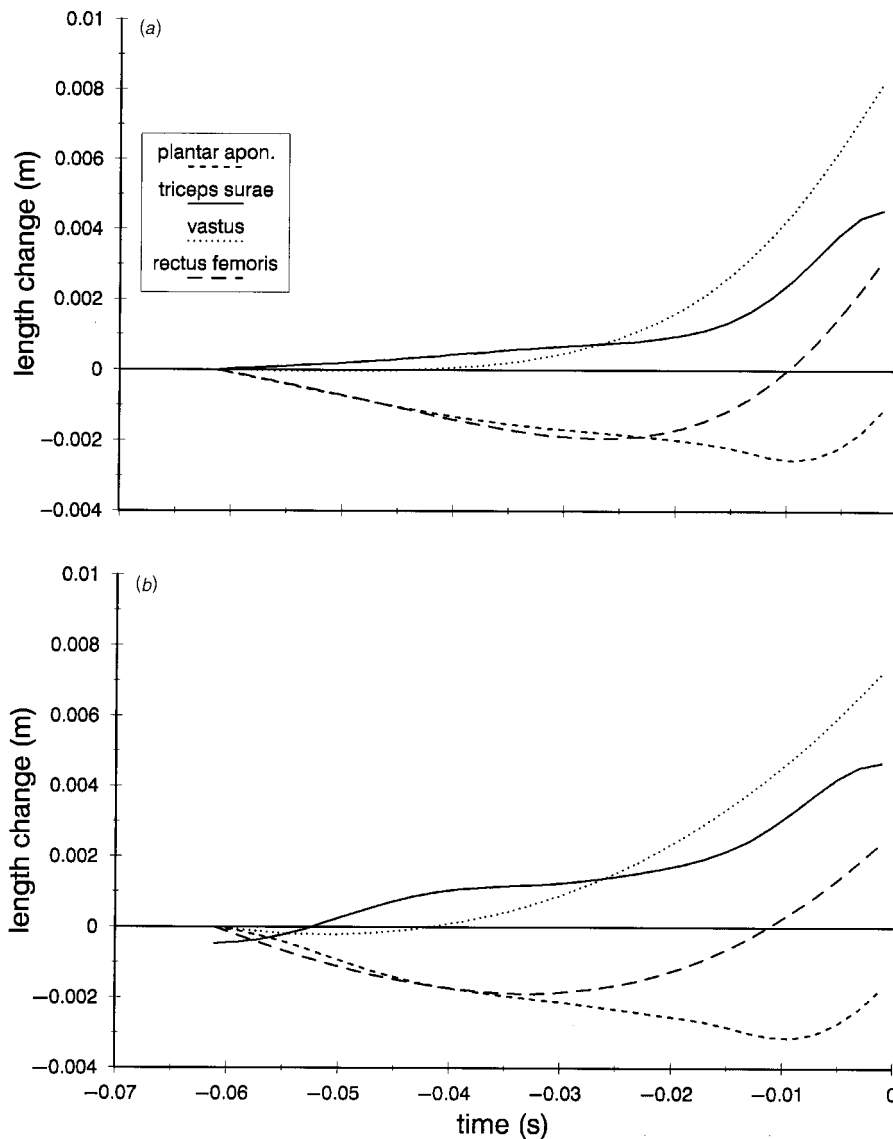
Figure 8. (*a*) Estimated tension over the considered muscle–tendon complexes for jump J33. The arrow points at the instant at which the total power requirements peak. (*b*) As in (*a*) but for jump J26.

obligatory because the contractile components alone are likely only to be able to deliver a fraction of the actual power requirements (see previous paragraphs). Structurally, the vastus muscle corresponds to the paradigm of a power amplifier: it is a multi-pinnate muscle with several well-developed internal and external aponeurotic tendon sheets either attaching to the femur shaft or merging into the patellar tendon. Functionally, it can fulfil this role when the next three conditions are met: (i) the connective tissue structures have the appropriate stiffness so that they can be extended (i.e. storing strain energy) by the occurring forces; (ii) the tension on the system increases to allow the extension; and (iii) an abrupt drop of the tension on the muscle–tendon complex occurs allowing power amplification (as the connective tissue structures recoil and convert the initially stored strain energy to work at a rate (i.e. power) similar to that of the tension decrease).

(i) *Appropriate stiffness*

Information about stiffness of the complex aponeurotic system of the vastus muscle is not available. Scott & Loeb (1995) showed that, within a muscle, internal aponeurosis

stiffness is similar to that of the external tendon. Making use of an average Young's modulus for mammalian tendon (about 1.5 GPa, cf. Ker (1992); Herzog & Loitz 1994) and assuming an 8% extension (Alexander 1988; Herzog & Loitz 1994) at peak load (about 500 N for J33), a cross-sectional surface of the tendon structures of 4.16 mm^2 (for both legs) can be calculated. Measuring the width and depth of the patellar tendon of the dissection specimen and applying isometric scaling (see § 2) reveals a surprisingly close estimate for the cross-sectional surface of 4.22 mm^2 for specimen 1 (an elliptic cross-section is assumed). Therefore, it is assumed that this condition is fulfilled.

(ii) *Increasing tension*

The only EMG-recording available to date for jumping in bushbabies (a telemetric surface-EMG of the vastus lateralis muscle for two jumps by one specimen with a 10%-body-weight load attached to the back; Günther 1989) shows that activity of the vastus muscle starts during crouching and ceases immediately before the peak in the ground reaction force is reached. This points to potential loading of the series elastic component of the knee extensors with strain energy during the crouching
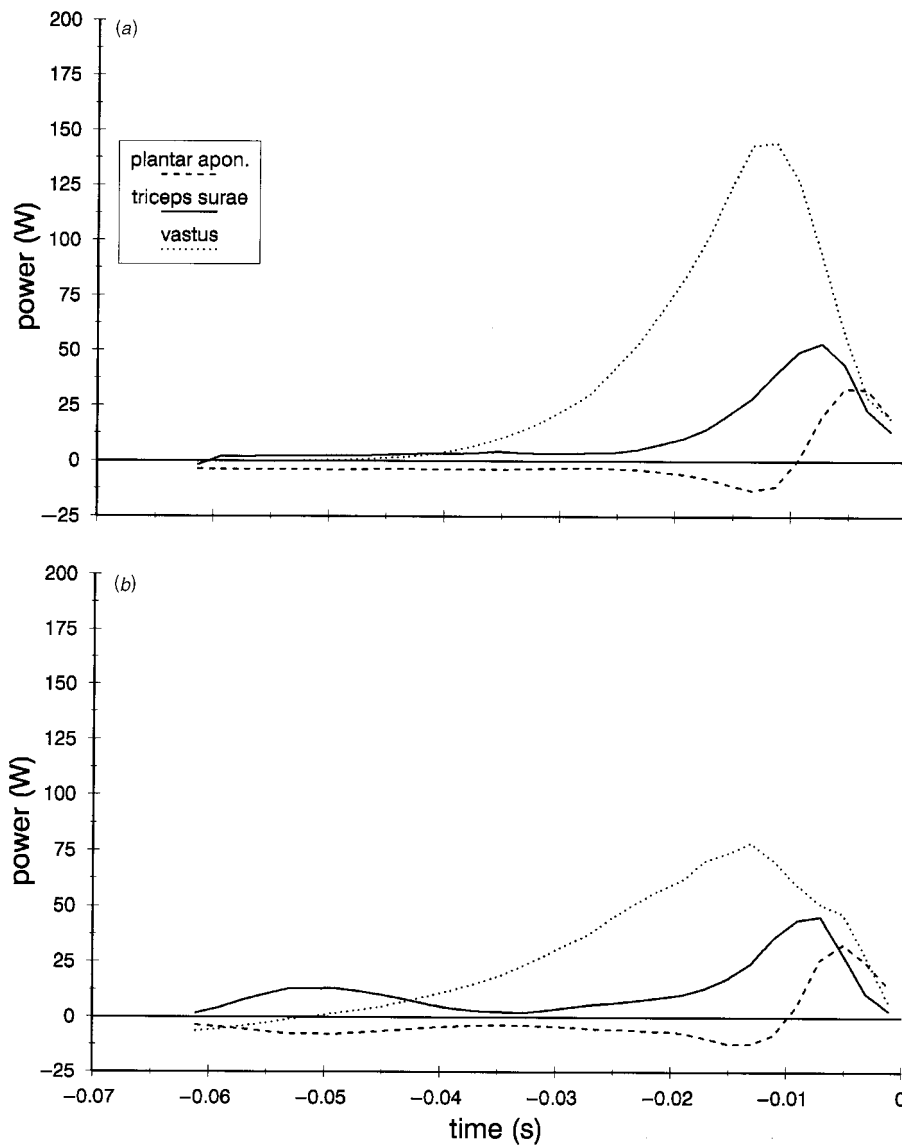
Figure 9. (*a*) Power output of the considered muscle–tendon complexes for jump J33 (internal power). (*b*) As in (*a*) but for jump J26.

phase. However, initial energy storage should rely on activity of the knee flexors during the countermovement because gravitational forces alone can be assumed to be too small for an active pre-stretch of the vastus muscle–tendon complex (cf. the small body mass; see also Alexander 1995). The countermovement, however, is not immediately followed by knee extension (figure 3*b*; knee extension starts about halfway through the push-off) and tension of the vastus may not therefore decline before extension actually starts if the stored energy has to be used. This condition is fulfilled when activity of the bi-articular hamstrings involved in hip extension (and probably reactive forces from the upwards-accelerating trunk as well) prevents the knee from being extended untimely and allows for further force development by the vastus muscle bundles. Such an activity pattern was experimentally found for cats jumping vertically towards a target (Zajac 1985). The technique in maximal jumping (up to 1.6 m) is closely comparable to that of the bushbaby. Extending movements are initiated by the backwards rotation of the trunk from a crouched (horizontal) position. Next, propulsion is dominated by quick hind-limb extension while trunk rotation continues (compare

with figure 3*b*). Integrated EMG-data prove that the activity of the bi-articular hamstrings is high in the first phase, but ceases when leg extension starts. Hip extension is then further powered by the mono-articular extensors (Zajac 1985, fig. 6). Therefore it seems plausible that energy storage proceeds during the first half of the push-off, when the knees are still fully flexed. Furthermore, figure 8 shows that the tension of the vastus muscle–tendon complex keeps on rising considerably (up to a 50% increase) until the last 13 ms of knee extension. This implies that muscle fibres not only work to extend the knee (and the ankle and midfoot via the triceps coupling) but also to stretch its connective tissue sheets by loading them further with strain energy.

(iii) *Abrupt tension drop*

During the last 13 ms of the push-off (i.e. immediately before peak ground reaction forces occur; figure 3*a*), the geometric model output of the vastus muscle–tendon complex shows the fast tension decline (figure 8) required for the rapid recoil of the tensed connective tissue sheets and the inherent high power output. The rate of decline in tension will be highest when neuronal stimulation of

the muscle ceases entirely at the appropriate time (a relaxation time of 13 ms is short, but feasible for fast glycolitic fibres of warm-blooded animals; cf. Woledge *et al.* 1995). It is, therefore, remarkable that the offset of the vastus-EMG (Günther 1989) coincides precisely with the onset of the tension decline, namely just before the ground reaction force peaks (see previous paragraph). Furthermore, the instant of maximum power requirements for the jump occurs in the middle of the 'fast-decline phase' of the vastus muscle (arrows on figure 8, compare with figure 6). If it is agreed that the ultimate shortening of the vastus muscle–tendon complex represents tendon recoil, a rough estimate of the energy storage and power amplification can be made. For linear elastic structures (such as tendons, cf. Alexander (1988); Ker 1992) energy storage equals the product of maximum force and maximum extension divided by two. Maximum force is given by the model output (figure 8) and maximum extension equals the muscle–tendon shortening during the 'tension decline phase'. Based on figures 7 and 8, this maximum extension can be estimated to about 5 mm. This is calculated to be a storage of 1.2 J and 0.83 J for J33 and J26, respectively. As this energy is freed during the last 13 ms the average power output (work–time) from the connective tissue structures equals 92 W and 64 W, respectively. These contributions seem reasonable considering the requirements for jumping by bushbabies. Provided that the storage of this energy starts at the onset of the EMG-activity of the vastus (about 200 ms before take-off; see Günther 1989), loading of the tendon structures takes about 15 times longer than the recoil and an equal amplification factor can be assumed.

However, one condition must be met so that the postulated key role of the knee extensor muscle tendon system in the *Galago*'s jumping mechanism can be applied: the force requirements, as they are predicted by the model, must be actually feasible for the vastus muscle. Using the allometric equations of Alexander *et al.* (1981), I calculated an average fibre length of 8.5 mm and 9.2 mm for the quadriceps muscle (vastus plus rectus femoris) of specimens 1 and 2, respectively. This was confirmed by rough estimates on longitudinal sections through preserved vastus muscle bundles (vastus lateralis lateralis; vastus lateralis medialis and vastus medialis) which gave an average length of 11 mm (for *Galago crassicaudatus*, the larger thick-tailed bushbaby, a length of 14 mm was determined; original data of Alexander *et al.* (1981); R. McN. Alexander, personal communication). Taking into account that the vastus muscles amount to 12.5% of the total body mass (both sides of the body) and making use of a muscle density of 1050 kg m^{-3} (Taylor 1994) and a muscle stress of 25 N cm^{-2} (Herzog 1994), I calculated the potential maximum isometric force of the knee extensors to be 879 N (sp.1) and 989 N (sp.2) (perpendicular to the muscle fibres). This is well above the required peak forces estimated by means of the muscle–tendon model (480 and 332 N, respectively; see figure 8) even if one accounts for muscle pinnation.

Such values only refer to muscles acting at the plateau of the length–tension curve, but experiments on fish and frog muscle suggest that muscle design is adapted in such a way that physiological working ranges correspond to optimal myofilament overlap (see, for example, Rome 1994; Lutz & Rome 1994). However, given the short muscle-fibre length and the fact that the vastus muscle–tendon complex has to shorten about 18% to extend the knee for jumping (see also Hall-Craggs 1974), it is questionable whether this holds for the vastus muscle too. Data on length–tension relations at the sarcomere level, integrated with the actual working ranges of the fibres, are not available for the vastus muscle of the bushbaby. But, the multi-pinnate nature of the muscle implies that a given fibre shortening corresponds to a larger tendon displacement (or extension) owing to the involved change of the pinnation angle (e.g. about 25% increase for a 30° pinnate fibre shortening along its plateau; see, for example, Alexander 1983). Furthermore, the length–tension relation established for the entire vastus muscle (nerve stimulation: Hall-Craggs 1974) shows an extended plateau which covers about one-third of the active length change of the vastus muscle–tendon complex. This corresponds to 50% of the angular displacement of the knee (compare figures 7 and 3*b*).

Muscle force also depends on the shortening speed of its fibres. When the second-half (and at the same time the fastest phase; within 13 ms) of the knee extension relies on elastic recoil of tendon structures, the contraction of the muscle fibres for aponeurosis lengthening and initial knee extension can be spread over a period ranging from the crouching phase to the instant of the sudden tension drop (off-set of the activation). Therefore, shortening velocity of the muscle fibres can be assumed to be fairly low. Furthermore, as fibre pinnation causes an increased tendon displacement (or extension; see previous paragraph), the shortening velocity of the fibres is lower than the speed of the tendon structures.

These considerations about maximum force capabilities, and the influence of length changes and shortening velocity relations, support the prediction that the vastus muscle can sustain the required high, and increasing, force output.

A role could not be found for the bi-articular rectus femoris muscle, which shares the patellar tendon with the vastus muscle for its insertion. However, Jacobs *et al.* (1996) showed that, in human jumping, this muscle transports a considerable amount of energy (21%) from the extending hip to the knee. This compares to the power transport function described for the bi-articular calf muscles. In *Galago*, the rectus femoris muscle is slender (only about 1.1% of the total leg muscle mass) but very tendinous. Straightforward calculation of its mechanical behaviour in jumping is impeded by the indeterminacy problem, but it is probable that the muscle fulfils a similar role as that described for humans. Furthermore, the length estimates by means of the geometric model show that the rectus femoris lengthens during the push-off, until rapid extension of the knee starts (see § 3 and figure 7). Then fast shortening occurs at a rate similar to that of the vastus muscle–tendon complex. This suggests that energy delivered by the hip extensors in an early phase of the push-off may be stored temporarily in the tendinous rectus femoris muscle to be used later for knee extension. The discrepancy between the extension and shortening phases (about 80 ms against 20 ms) may also indicate a moderate power amplification. Unfortunately, precise figures that could reveal the importance of the

rectus femoris in the jump of the *Galago* could not be calculated.

4. GENERAL CONCLUSIONS

These arguments suggest that the vastus muscle–tendon system drives maximal jumping in bushbabies in a complex way. Energy is first stored by active pre-stretching during crouching and initial hip extension. Then, during most of the knee extension, the internal and external aponeurotic tendon sheets are further loaded with about an equal amount of energy (as shown by the force levels). All this strain energy is suddenly released late in the push-off, likely triggered by the abrupt switch-off of the motor drive of the knee extensors. The involved power output is complemented by direct muscle power. In this way, maximal jumping in bushbabies can be interpreted as a sequential combination of 'countermovement', 'catapult' and 'squat-jumping with compliant tendons' according to Alexander's (1995) model. Substantial power amplification is likely achieved. Structurally, the amplifier seems to be principally located in the large vastus muscle–tendon complex. The work done by this muscle–tendon complex is not only used to extend the knee, but energy is also transmitted down the leg to participate in ankle and midfoot extension.

REFERENCES

Alexander, R. McN. 1983 *Animal mechanics*, 2nd edn. Oxford: Blackwell.

Alexander, R. McN. 1988 *Elastic mechanisms in animal movement*. Cambridge University Press.

Alexander, R. McN. 1992 *Exploring biomechanics, animals in motion*. New York: The Scientific American Library.

Alexander, R. McN. 1995 Leg design and jumping technique for humans, other vertebrates and insects. *Phil. Trans. R. Soc. Lond.* B **347**, 235–248.

Alexander, R. McN. & Bennet-Clark, H. C. 1977 Storage of elastic strain energy in muscle and other tissue. *Nature* **265**, 114–117.

Alexander, R. McN., Jayes, A. S., Maloiy, G. M. O. & Wathuta, E. M. 1981 Allometry of the leg muscles of mammals. *J. Zool.* **194**, 539–552.

Bennet-Clark, H. C. 1976 Energy storage in jumping animals. In *Perspectives in experimental biology* (ed. D. P. Spencer), pp. 467–479. Oxford: Pergamon Press.

Bennet-Clark, H. C. 1977 Scale effects in jumping animals. In *Scale effects in animal locomotion* (ed. T. J. Pedley), pp. 185–201. London: Academic Press.

Bobbert, M. F., Huying, P. A. & Van Ingen Schenau, G. J. 1986*a* A model of the human triceps surae muscle–tendon complex applied to jumping. *J. Biomech.* **19**, 887–898.

Bobbert, M. F., Huying, P. A. & Van Ingen Schenau, G. J. 1986*b* An estimation of the power output and work done by the human triceps surae muscle–tendon complex in jumping. *J. Biomech.* **19**, 899–906.

Crompton, R. H., Sellers, W. I. & Günther, M. M. 1993 Energetic efficiency and ecology as selective factors in the saltatory adaptation of prosimian primates. *Proc. R. Soc. Lond.* B **254**, 41–45.

Demes, B. & Günther, M. M. 1989 Biomechanics and allometric scaling in primate locomotion and morphology. *Folia Primatol.* **53**, 125–141.

Emerson, S. B. 1985 Jumping and leaping. In *Functional vertebrate morphology* (ed. M. Hildebrand, D. M. Bramble & K. F. Liem), pp. 58–72. Cambridge, MA: Belknap Press.

Enoka, R. M. 1994 *Neuromechanical basis of kinesiology*, 2nd edn. Champaign, IL: Human Kinetics.

Grand, T. I. 1977 Body weight: its relation to tissue composition segment distribution and motor function. 1. Interspecific comparison. *Am. J. Phys. Anthrop.* **47**, 211–240.

Günther, M. M. 1985 Biomechanische Voraussetzungen beim Absprung des Senegalgalagos. *Z. Morph. Anthrop.* **75**, 287–306.

Günther, M. M. 1989 Funktionsmorphologische Untersuchungen zum Springverhalten an mehreren Halbaffenarten. PhD thesis, University of Berlin (BRD), Germany.

Günther, M. M. & Niemitz, C. 1982 Comparative analyses of the leap in three primate species. *Verh. Anat. Ges.* **76**, 615–616.

Günther, M. M., Ishida, H., Kumakura, H. & Nakano, Y. 1991 The jump as a fast mode of locomotion in arboreal and terrestrial biotopes. *Z. Morph. Anthrop.* **78**, 341–372.

Günther, M. M., Preuschoft, H., Ishida, H. & Nakano, Y. 1992 Can prosimian-like leaping be considered a preadaptation to bipedal walking in hominids? In *Topics in primatology*, vol. 3 (ed. S. Matano, R. H. Tuttle, H. Ishida & M. Goodman), pp. 153–165. Tokyo University Press.

Hall-Craggs, E. B. C. 1964 The jump of the bushbaby—a photographic analysis. *Med. Biol. Illust.* **14**, 170–174.

Hall-Craggs, E. B. C. 1965 An analysis of the jump of the lesser galago (*Galago senegalensis*). *J. Zool.* **147**, 20–29.

Hall-Craggs, E. B. C. 1966 Muscle tension relationships in *Galago senegalensis*. *J. Anat.* **100**, 699–700.

Hall-Craggs, E. B. C. 1974 Physiological and histochemical parameters in comparative locomotor studies. In *Prosimian biology* (ed. R. D. Martin, G. A. Doyle & A. C. Walker), pp. 831–845. London: Duckworth.

Herzog, W. 1994 Muscle. In *Biomechanics of the musculo-skeletal system* (ed. B. M. Nigg & W. Herzog), pp. 154–190. Chichester, UK: Wiley.

Herzog, W. & Loitz, B. 1994 Tendon. In *Biomechanics of the musculo-skeletal system* (ed. B. M. Nigg & W. Herzog), pp. 133–153. Chichester, UK: Wiley.

Jacobs, R., Bobbert, M. F. & Van Ingen Schenau, G. J. 1996 Mechanical output from individual muscles during explosive leg extensions: the role of biarticular muscles. *J. Biomech.* **29**, 513–523.

Jouffroy, F. K. 1989 Quantitative and experimental approaches to primate locomotion, a review of recent advances. In *Perspectives in primate biology*, vol. 2 (ed. P. K. Seth & S. Seth), pp. 47–108. New Delhi: Today & Tomorrow's Printers & Publishers.

Jouffroy, F. K. & Gasc, J. P. 1974 A cineradiographical analysis of leaping in an African prosimian (*Galago alleni*). In *Primate locomotion* (ed. J. A. Jenkins), pp. 117–142. London: Academic Press.

Jouffroy, F. K. & Günther, M. M. 1985 Interdependence of morphology and behavior in the locomotion of galagines. In *Primate morphophysiology, locomotor analyses and human bipedalism* (ed. S. Kondo), pp. 201–234. Tokyo University Press.

Jouffroy, F. K., Gasc, J. P., Décombas, M. & Oblin, S. 1974 Biomechanics of vertical leaping from the ground in *Galago alleni*: a cineradiographic analysis. In *Prosimian biology* (ed. R. D. Martin, G. A. Doyle & A. C. Walker), pp. 817–827. London: Duckworth.

Ker, R. F. 1992 Tensile fibres: strings and straps. In *Biomechanics, materials, a practical approach* (ed. J. F. V. Vincent), pp. 75–98. Oxford: IRL Press.

Komi, P. V. 1992 *Strength and power in sport*. London: Blackwell.

Lutz, G. J. & Rome L. C. 1994 Built for jumping: the design of the frog muscular system. *Science* **263**, 370–372.

Marsh, R. L. & John-Alder, H. B. 1994 Jumping performance of hylid frogs measured with high-speed cine film. *J. Exp. Biol.* **188**, 131–141.

Nigg, B. M. & Herzog, W. 1994 *Biomechanics of the musculo-skeletal system*. Chichester, UK: Wiley.

Pennycuick, C. J. & Parker, G. A. 1966 Structural limitations on the power output of the pigeon's flight muscles. *J. Exp. Biol.* **45**, 489–498.

Plompen, H. 1992 Biomechanische analyse van de verticale sprong van *Galago senegalensis*. Licence Thesis, University of Antwerp (Be; in Dutch).

Plompen, H., Aerts, P., De Clercq, D. & De Vree, F. 1992 Biomechanical analysis of the vertical jump of *Galago senegalensis*. *Belg. J. Zool.* **122**, 241.

Rome, L. C. 1994 The mechanical design of the fish muscular system. In *Mechanics and physiology of animal swimming* (ed. L. Maddock, Q. Bone & J. M. V. Rayner), pp. 75–98. Cambridge University Press.

Scott, S. H. & Loeb, G. E. 1995 Mechanical properties of aponeurosis and tendon of the cat soleus muscle during whole-muscle isometric contractions. *J. Morph.* **224**, 73–86.

Sellers, W. I. 1992 A study of leaping in prosimian primates. PhD thesis, University of Liverpool, UK.

Sickels, D. W. & Pinkstaff, C. A. 1981 Comparative histochemical study of prosimian primate hindlimb muscles. II. Populations of fiber types. *Am. J. Anat.* **160**, 187–194.

Smith, R. M. 1987 Biomechanics of the locomotion of *Galago senegalensis*. PhD thesis, Arizona State University, USA.

Stevens, J. L., Edgerton, R. & Mitton, S. 1971 Gross anatomy of the hindlimb skeletal system of the *Galago senegalensis*. *Primates* **12**, 313–321.

Stevens, J. L., Edgerton, R. & Mitton, S. 1972 Gross anatomy of the hindlimb skeletal muscles of the *Galago senegalensis*. *Primates* **13**, 83–101.

Stevens, J. L., Edgerton, R. V., Haines, D. E. & Meyer, D. M. 1981 An atlas and source book of the lesser bushbaby, *Galago senegalensis*. Boca Raton: CRC Press.

Taylor, M. A. 1994 Stone, bone or blubber? Buoyancy control strategies in aquatic tetrapods. In *Mechanics and physiology of animal swimming* (ed. L. Maddock, Q. Bone & J. M. V. Rayner), pp. 151–162. Cambridge University Press.

Van Leeuwen, J. L. 1992 Muscle function in locomotion. In *Advances in comparative and environmental physiology. 11. Mechanics of animal locomotion* (ed. R. McN. Alexander), pp. 191–250. Berlin: Springer.

Winter, D. A. 1990 *Biomechanics and motor control of human movement*, 2nd edn. New York: Wiley.

Woledge, R. C., Curtin, N. A. & Homsher, E. 1985 *Energetic aspects of muscle contraction*. London: Academic Press.

Wood, G. A. 1982 Data smoothing and differentiation procedures in biomechanics. In *Exercise and sport sciences reviews*, vol. 10 (ed. R. L. Tur-jung), pp. 308–362. Baltimore, MD: Williams & Wilkins.

Zajac, F. E. 1985 Thigh muscle activity in cats during maximal height jumps. *J. Neurophysiol.* **53**, 979–993.

Zajac, F. E. & Gordon, M. E. 1989 Determining muscle's force and action in multi-articular movement. In *Exercise and sport science reviews*, vol. 17 (ed. K. Pandolf), pp. 187–230. Baltimore, MD: Williams & Wilkins.

Zernicke, R. F. & Smith, L. J. 1996 Biomechanical insights into neural control of movement. In *The handbook of physiology* (ed. L. Rowell & J. Shepard), pp. 293–330. New York: Oxford University Press.